# Association structures of ionic liquid/DMSO mixtures studied by high-pressure infrared spectroscopy

Jyh-Chiang Jiang, Kuan-Hung Lin, Sz-Chi Li, Pao-Ming Shih, Kai-Chan Hung, Sheng Hsien Lin, and Hai-Chou Chang

Citation: The Journal of Chemical Physics **134**, 044506 (2011); doi: 10.1063/1.3526485
View online: http://dx.doi.org/10.1063/1.3526485
View Table of Contents: http://scitation.aip.org/content/aip/journal/jcp/134/4?ver=pdfcov
Published by the AIP Publishing

# Association structures of ionic liquid/DMSO mixtures studied by high-pressure infrared spectroscopy

Jyh-Chiang Jiang,[1] Kuan-Hung Lin,[2] Sz-Chi Li,[2] Pao-Ming Shih,[2] Kai-Chan Hung,[2] Sheng Hsien Lin,[3,4] and Hai-Chou Chang[2,a)]
[1]*Department of Chemical Engineering, National Taiwan University of Science and Technology, Taipei 106, Taiwan*
[2]*Department of Chemistry, National Dong Hwa University, Shoufeng, Hualien 974, Taiwan*
[3]*Department of Applied Chemistry, National Chiao Tung University, Hsinchu 30010, Taiwan*
[4]*Institute of Atomic and Molecular Sciences, Academia Sinica, P.O. Box 23-166, Taipei 106, Taiwan*

(Received 1 March 2010; accepted 18 November 2010; published online 24 January 2011)

Using high-pressure infrared methods, we have investigated close interactions of charge-enhanced C–H–O type in ionic liquid/dimethyl sulfoxide (DMSO) mixtures. The solvation and association of the 1-butyl-3-methylimidazolium tetrafluoroborate ($BMI^+BF_4^-$) and 1-butyl-2,3-dimethylimidazolium tetrafluoroborate ($BMM^+BF_4^-$) in DMSO-$d_6$ were examined by analysis of C–H spectral features. Based on our concentration-dependent results, the imidazolium C–H groups are more sensitive sites for C–H–O than the alkyl C–H groups and the dominant imidazolium C–H species in dilute ionic liquid/DMSO-$d_6$ should be assigned to the isolated (or dissociated) structures. As the dilute mixtures were compressed by high pressures, the loss in intensity of the bands attributed to the isolated structures was observed. In other words, high pressure can be used to perturb the association–dissociation equilibrium in the polar region. This result is remarkably different from what is revealed for the imidazolium C–H in the $BMM^+BF_4^-/D_2O$ mixtures. DFT-calculations are in agreement with our experimental results indicating that $C^4$–H–O and $C^5$–H–O interactions seem to play non-negligible roles for $BMM^+BF_4^-$/DMSO mixtures. © *2011 American Institute of Physics*. [doi:10.1063/1.3526485]

## I. INTRODUCTION

Ionic liquids show some interesting features, such as negligible vapor pressure, ability of dissolving a variety of chemicals, and wide liquid range.[1–8] Their quite rapid emergence as alternative solvents has involved chemical reactions, liquid–liquid extractions, battery electrolytes, and gas storage, to mention just a few examples.[1,2] Research exploring the uses of ionic liquids is growing at an exponential pace. However, one of the barriers in the application of ionic liquids is the general lack of physical property data for these compounds toward fundamental understanding of the system. The physical and chemical properties of ionic liquids can be fine-tuned through the selection of their cation and anion moieties.[1,2] Consequently, ionic liquids can be made compatible with a wide range of materials. An important issue in the structures of ionic liquids is the relative geometry between the anion and cation comprising the bulk liquid, while the type of anion acts a significant role in the structural changes.[2]

Ionic liquids can be employed together with other solvents, which may affect their properties. Properties of binary liquid mixtures have been extensively studied to understand the nature and extent of various intermolecular interactions existing between different species present in the mixtures. Of particular interest are the effects of water and numerous studies on ionic liquid/water systems have been made.[9–15] Compared with the intensive investigations on the ionic liquid/water mixtures, there have been a few reports on solvation behavior of ionic liquid in nonaqueous molecular liquids.[16–20] In this contribution, we present a means of looking at physicochemical properties of ionic liquid/dimethyl sulfoxide (DMSO) mixtures, by using variable pressures as a window into the nature of charge-enhanced C–H–O interactions.

Among the common ionic liquids developed, the imidazolium-type ionic liquids derived from 1-alkyl-3-methyl imidazolium cations in association with weakly coordinating anions represent the most popular in many applications.[1,2,21,22] With three hydrogen atoms bound to the imidazolium ring, two or three resolved absorption bands are observed with 1-alkyl-3-methylimidazolium salts in the IR spectral region between 3000 and 3200 $cm^{-1}$. These can be attributed to coupled aromatic C–H stretching vibrations. The relative acidity of the hydrogen atoms in the imidazolium ring is important for quantifying the effect of ionic liquids in the binary mixtures. The $C^2$ proton is the most acidic proton on the imidazolium ring and may form hydrogen bonds with the anions. However, there is also experimental evidence that imidazolium salts will, under certain conditions, prefer to bind to transition metals at $C^{4,5}$, that is the less-acidic sites.[23] In this article, we characterize the effect of hydrogen-atom substitution by methyl group at $C^2$ carbon of the imidazolium ring on the physical properties of ionic liquids based on the $BF_4^-$ anion.

One of the attractive features of the 1-alkyl-3-methylimidazolium cation is its inherently amphiphilic character as a surfactant. Both experiments and simulations have found that the alkyl side-chain length has an influence on the supramolecular assemblies of ionic liquids.[2,7,24] Alkyl

a)Author to whom correspondence should be addressed. Electronic mail: hcchang@mail.ndhu.edu.tw; Fax: +886-3-8633570; Tel. +886-3-8633585.

 

imidazolium cations with long enough alkyl chain length ($n \geq 4$) were characterized by the existence of structural organization at the nanometer scale, as reported by Triolo *et al*.[24] Studies were carried out to investigate the formation of associated species such as ion pairs and aggregates in ionic liquid mixtures.[25–28] The existence of a critical aggregation concentration (CAC) for imidazolium has been investigated in water and in organic solvents using several experimental techniques.

Knowledge of the nature and strength of hydrogen bonding interactions is fundamental to understand the physical properties of ionic liquids. The hydrogen bonding interactions are complex for aqueous ionic liquids with varying anions, due to pronounced anion–water interactions. However, some research groups infer the non-negligible role of cation–water interactions.[29,30] Miscibility of imidazolium-based ionic liquids with water depend on the side chain lengths at the cation.[30] As this changes the solubility behavior, the cation may have some implications on the water–ionic liquid interactions. Various studies have been performed to elucidate the role of weak hydrogen bonds, such as C–H–O and C–H–X, in the structure of ionic liquids.[29,31–33] The cation–water interaction was deduced by Mele *et al*. from ROESY spectra.[29] One of the intriguing aspects of weak hydrogen bonds is that the C–H covalent bond tends to shorten as a result of formation of a hydrogen bond with a Lewis base. Hobza *et al*. suggested that the strengthened C–H bond originates from the electron density transfer from the proton acceptor to the remote part of the proton donor.[34] Scheiner[35] and Dannenberg,[36] however, view conventional and C–H–O hydrogen bonds to be very similar in nature. The origin of both the red- and blue-shifted hydrogen bonds was concluded to be the same by the Schlegel group[37] and the Hermansson group.[38] One of the underlying reasons for this debate is the weakness of C–H–O interactions. The study of methods that enhance C–H–O interactions is crucial if we are to obtain further details of this important phenomenon. In this study, we present a means of looking at this phenomenon, by using variable pressure as a window into the nature of charge enhanced C–H–O interactions.

Changing the temperature of a chemical system at ambient pressure produces a simultaneous change in thermal energy and volume. To separate the thermal and volume effects, one must perform high-pressure experiments. Static pressures up to several megabars can be generated using diamond anvil cells. Nevertheless, the pressures used to investigate chemical systems typically range from ambient to several GPa. The static approach is of interest because it allows continuous tuning of the pressure and the possibility to employ a large number of probing techniques that allow *in situ* measurements. In this article, we report how *in situ* high-pressure infrared spectroscopy using a diamond anvil was applied to ionic liquid mixtures.

## II. EXPERIMENTAL

Samples were prepared using 1-butyl-3-methylimidazolium tetrafluoroborate ($BMI^+BF_4^-$ >97%, Fluka), 1-butyl-2,3-dimethylimidazolium tetrafluoroborate ($BMM^+BF_4^-$ >99%, Fluka), DMSO-$d_6$ (99.9 at. % D, Aldrich), and $D_2O$ (99.9% D, Aldrich). A diamond anvil cell (DAC) of Merril–Bassett design, having a diamond culet size of 0.6 mm, was used for generating pressures up to ca. 2 GPa. Two type-IIa diamonds were used for mid-infrared measurements. The sample was contained in a 0.3-mm-diameter hole in a 0.25-mm-thick inconel gasket mounted on the diamond anvil cell. To reduce the absorbance of the samples, $CaF_2$ crystals (prepared from a $CaF_2$ optical window) were placed into the holes and compressed firmly prior to inserting the samples. A droplet of a sample filled the empty space of the entire hole of the gasket in the DAC, which was subsequently sealed when the opposed anvils were pushed toward one another. Infrared spectra of the samples were measured on a Perkin-Elmer Fourier transform spectrophotometer (model Spectrum RXI) equipped with a lithium tantalite (LITA) mid-infrared detector. The infrared beam was condensed through a 5× beam condenser onto the sample in the diamond anvil cell. Typically, we chose a resolution of 4 $cm^{-1}$ (data point resolution of 2 $cm^{-1}$). For each spectrum, typically 1000 scans were compiled. To remove the absorption of the diamond anvils, the absorption spectra of DAC were measured first and subtracted from those of the samples. Pressure calibration follows Wong's method.[39,40] Spectra of samples measured at ambient pressure were taken by filling the samples in a cell having two $CaF_2$ windows but lacking the spacers.

The Raman spectra were measured using a 100 mW diode pumped solid state laser ($\lambda = 532$ nm) and a microscopic based Raman spectrometer having a 300 mm spectrograph (Acton SP308) and a side window photon counting detector system. Two type-Ia diamonds were used for Raman measurements

## III. RESULTS AND DISCUSSION

The infrared spectrum of pure1-butyl-3-methylimidazolium tetrafluoroborate ($BMI^+BF_4^-$) exhibits five discernible peaks, i.e., 2877, 2939, 2964, 3122, and 3162 $cm^{-1}$, respectively, in the 2800–3200 $cm^{-1}$ region. The absorption bands at 2877, 2939, and 2964 $cm^{-1}$ can be attributed to C–H stretching modes of the alkyl groups. The coupled imidazolium C–H stretching vibrations locate at 3122 and 3162 $cm^{-1}$. Figure 1 presents the concentration dependence of the maximum positions of the characteristic C–H bands of $BMI^+BF_4^-$ upon dilution with DMSO-$d_6$. Looking into more detail in Fig. 1, we observe no drastic changes in the concentration dependence of the alkyl C–H band frequency. In contrast with the trend observed for alkyl C–H stretches, the imidazolium C–H bands (Fig. 1) display anomalous concentration-induced frequency shifts as the $BMI^+BF_4^-$ is diluted. We observed no drastic changes in the imidazolium C–H band frequency at high concentration of $BMI^+BF_4^-$, that is 0.6 < mole fraction ($BMI^+BF_4^-$). This behavior may indicate a clustering of ionic liquid in polar region and a slight perturbation by the presence of DMSO-$d_6$ at high concentration. The imidazolium C–H absorption exhibits a decrease in frequency upon dilution at low concentration of ionic liquid, that is 0.6 > mole fraction ($BMI^+BF_4^-$). A possible explanation for this effect is the C–H–O interactions between imidazolium C–H groups and DMSO-$d_6$. The red-shifts of imidazolium C–H stretches

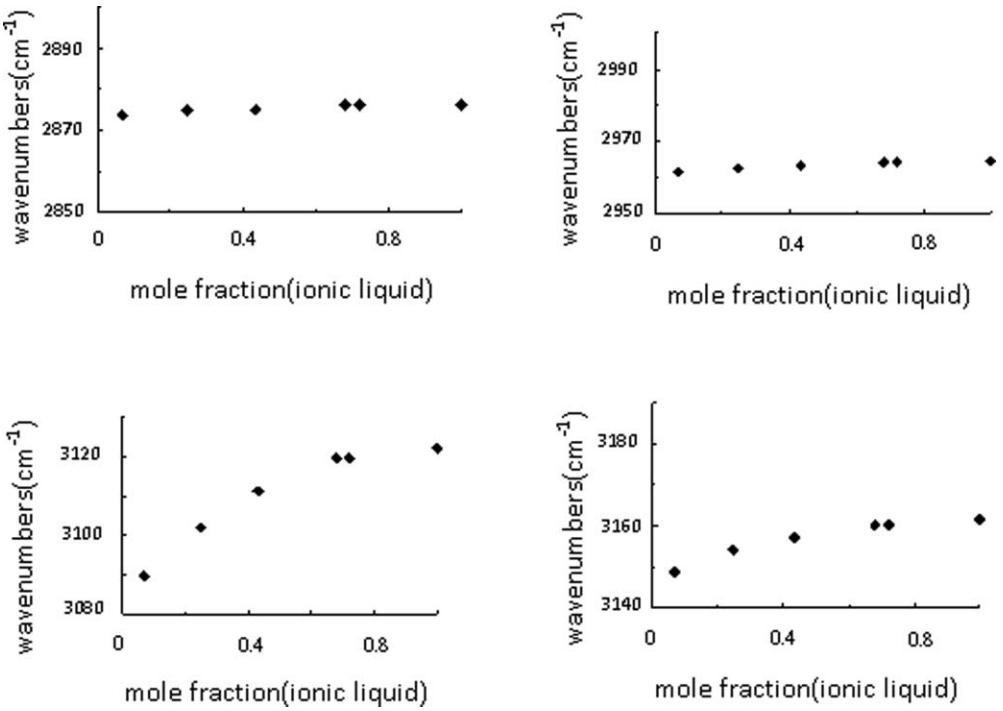


FIG. 1. Concentration dependence of the C–H stretching frequency of $BMI^+BF_4^-$/DMSO-$d_6$ versus the mole fraction of $BMI^+BF_4^-$.

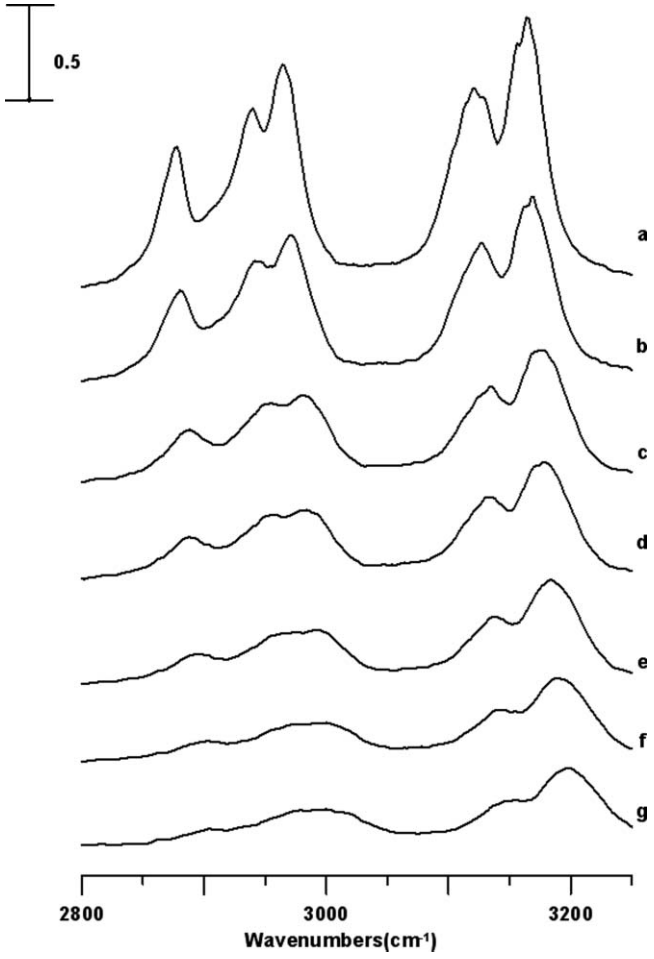


FIG. 2. Pressure dependence of IR spectra of pure $BMI^+BF_4^-$ under (a) ambient pressure and at (b) 0.3 GPa, (c) 0.9 GPa, (d) 1.5 GPa, (e) 1.9 GPa, (f) 2.3 GPa, and (g) 2.5 GPa.

observed in Fig. 1 may be due to the replacement of an interaction between the imidazolium C–H and an anion with an interaction with DMSO-$d_6$. Based on the results of Fig. 1, the imidazolium C–H groups seem to be more sensitive sites for C–H–O than the alkyl C–H groups. Several studies have suggested that ionic liquids tend to segregate into stable non-polar regions by aggregation of the alkyl groups for $C_4$ and longer and polar regions by charge ordering of the anions and imidazolium rings.[10,11,24] As shown in our previous reports, no appreciable changes in band frequency of the imidazolium C–H occurred as the $BMI^+BF_4^-$ was diluted by $D_2O$.[15] Nevertheless, the infrared absorption spectra of DMSO-$d_6$ mixtures exhibit a decrease in imidazolium C–H frequency upon dilution in Fig. 1. Thus, DMSO-$d_6$ can be added to significantly change the structural organization of $BMI^+BF_4^-$. Our results in Fig. 1 indicate that the presence of DMSO-$d_6$ perturbs the ionic liquid–ionic liquid associations in the imidazolium region.

Figure 2 presents infrared spectra of pure $BMI^+BF_4^-$ obtained under ambient pressure (curve a), and at 0.3 (curve b), 0.9 (curve c), 1.5 (curve d), 1.9 (curve e), 2.3 (curve f), and 2.5 GPa (curve g). As revealed in Figs. 2 and S1,[41] both the alkyl and imidazolium C–H stretching bands display nonmonotonic pressure dependences. They blue-shift initially [Figs. 2(a)–2(c)], then undergoes no change [Figs. 2(c) and 2(d)], and then blue-shift [Figs. 2(d)–2(g)] again as the pressure is elevated. This discontinuity in frequency shift in Figs. 2 and S1 is similar to the trend revealed in the pressure-dependent study of pure 1-butyl-3-methylimidazolium hexafluorophosphate ($BMI^+PF_6^-$). The frequency shifts may originate from the combined effect of the overlap repulsion enhanced by hydrostatic pressure, the phase transition, C–H–F contacts, and so forth.

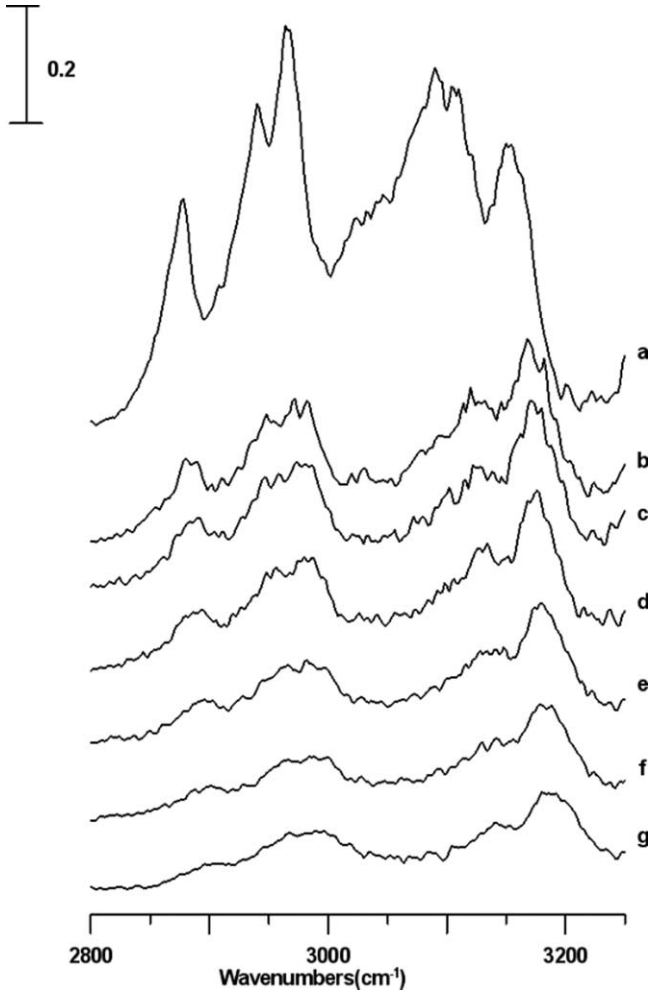


FIG. 3. IR spectra of a $BMI^+BF_4^-$/DMSO-$d_6$ mixture (mole fraction of $BMI^+BF_4^-$: ca. 0.15) obtained under ambient pressure (curve a) and at 0.3 GPa (curve b), 0.9 GPa (curve c), 1.5 GPa (curve d), 1.9 GPa (curve e), 2.3 GPa (curve f) and 2.5 GPa (curve g).

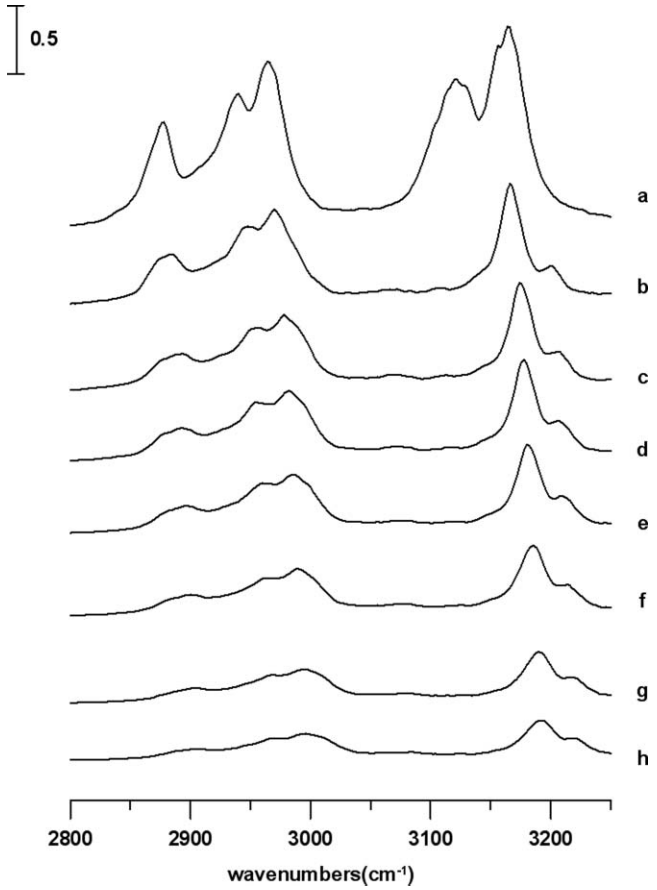


FIG. 4. IR spectrum of pure $BMI^+BF_4^-$ (curve a) and pressure dependence of IR spectra of pure $BMM^+BF_4^-$ under (b) ambient pressure and at (c) 0.3 GPa, (d) 0.9 GPa, (e) 1.5 GPa, (f) 1.9 GPa, (g) 2.3 GPa, and (h) 2.5 GPa.

Figure 3 displays the infrared spectra of a $BMI^+BF_4^-$/DMSO-$d_6$ mixture having its mole fraction of $BMI^+BF_4^-$ equal to 0.15 obtained under ambient pressure (curve a), and at 0.3 (curve b), 0.9 (curve c), 1.5 (curve d), 1.9 (curve e), 2.3 (curve f), and 2.5 GPa (curve g). The imidazolium C–H bands are red-shifted to 3091 and 3153 $cm^{-1}$ in Fig. 3(a) in comparison to the frequencies of 3122 and 3162 $cm^{-1}$, respectively, in Fig. 2(a). The broad features for imidazolium C–H absorption in Fig. 3(a) suggest the presence of at least two species, i.e., associated and isolated structures.[16,31,32] The associated species may be ion pairs or larger ion clusters and the isolated species may mean the dissociation into free ions or smaller ion clusters. Based on the concentration-dependent results in Fig. 1, the dominant imidazolium C–H species revealed in Fig. 3(a) should be assigned to the isolated (or dissociated) structure. As the sample was compressed to 0.3 GPa [Fig. 3(b)], the imidazolium C–H stretching modes in the region 3000–3250 $cm^{-1}$ underwent dramatic changes in their spectral profiles with bandwidth narrowing. The spectrum in Fig. 3(b) shows the imidazolium C–H stretching locating at 3121 and 3168 $cm^{-1}$, respectively. This behavior may be caused by the loss in intensity of the bands attributed to the isolated structures. In other words, the associated configuration is favored with increasing pressure by debiting the isolated form. The features of cation–anion interactions have attracted much attention recently, but the nature of the possible association is still under debate.[16,26–28] Therefore, the investigation of pressure effect on the association–dissociation transformation may be important to provide further clues. As revealed in Figs. 3(b)–3(g), the spectral features of the C–H stretching modes show further evolution upon compression through the observation of monotonic blueshifts in frequency. The associated form, being a less stable form for $BMI^+BF_4^-$/ DMSO-$d_6$ under ambient pressure [Fig. 3(a)], is switched to a more stable state under the condition of high pressures [Figs. 3(b)–3(g)].

We obtained a complementary insight into the C–H stretching spectral features revealed in Figs. 4(b)–4(h) by measuring the pressure-dependent variations in the infrared spectra of pure 1-butyl-2,3-dimethylimidazolium tetrafluoroborate ($BMM^+BF_4^-$). To see the differences of the spectra for $BMI^+BF_4^-$ and $BMM^+BF_4^-$, the IR spectrum of pure $BMI^+BF_4^-$ obtained at ambient pressure is also displayed in Fig. 4(a). As seen in Figs. 4(a) and 4(b), the imidazolium C–H absorptions undergo significant changes as the $C^2$ carbon has been methylated for $BMM^+BF_4^-$. Figures 4(b)–4(g) present infrared spectra of pure $BMM^+BF_4^-$ obtained under

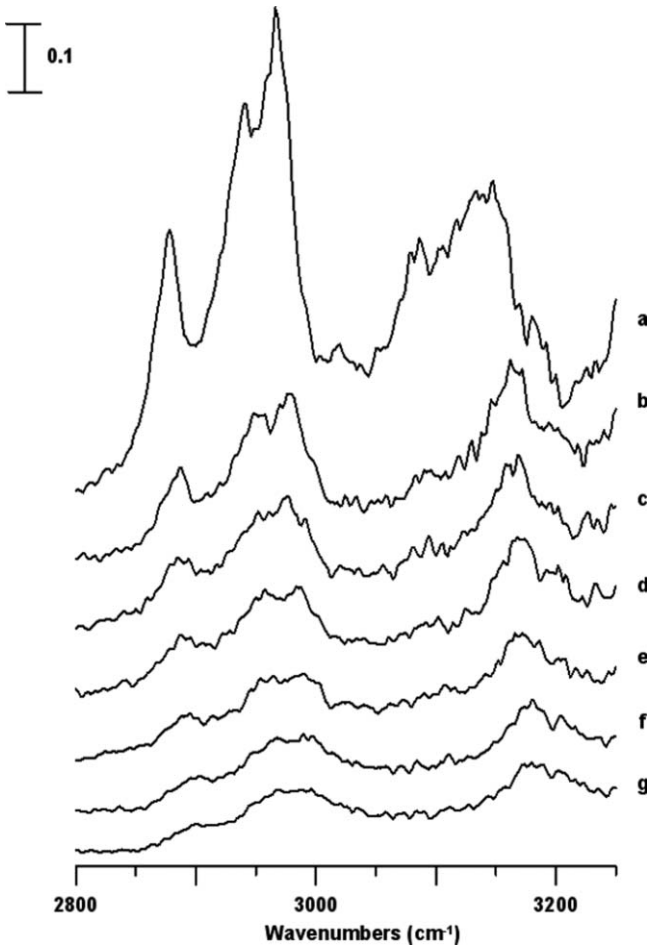


FIG. 5. IR spectra of a $BMM^+BF_4^-$/DMSO-$d_6$ mixture having mole fraction of $EMI^+TFSA^-$ equal to 0.14 obtained under ambient pressure (curve a) and at 0.3 GPa (curve b), 0.9 GPa (curve c), 1.5 GPa (curve d), 1.9 GPa (curve e), 2.3 GPa (curve f) and 2.5 GPa (curve g).

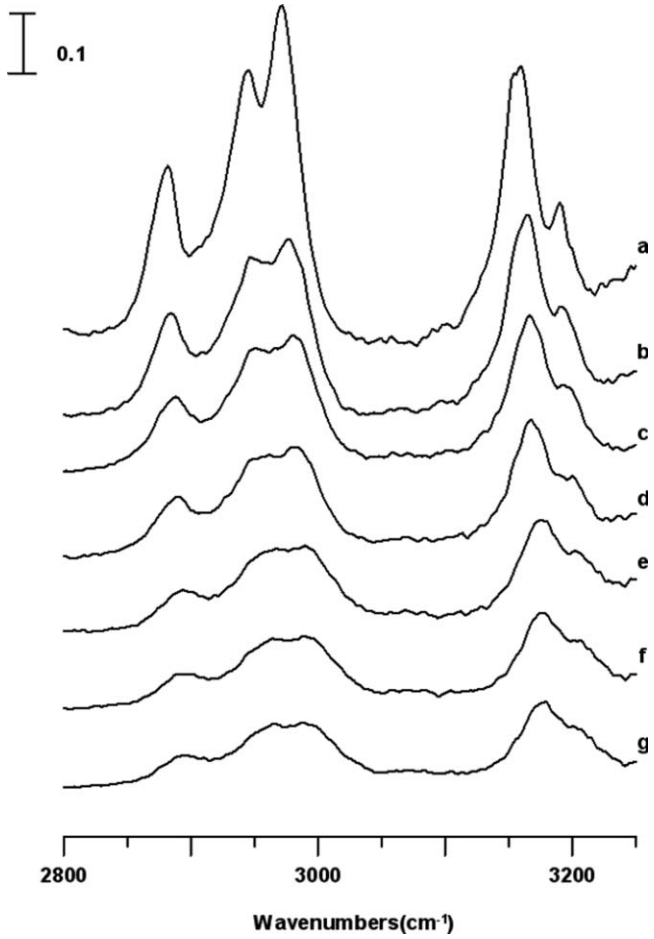


FIG. 6. IR spectra of a $BMM^+BF_4^-/D_2O$ mixture having mole fraction of $BMM^+BF_4^-$ equal to 0.06 obtained under ambient pressure (curve a) and at 0.3 GPa (curve b), 0.9 GPa (curve c), 1.5 GPa (curve d), 1.9 GPa (curve e), 2.3 GPa (curve f), and 2.5 GPa (curve g).

ambient pressure (curve b), and at 0.3 (curve c), 0.9 (curve d), 1.5 (curve e), 1.9 (curve f), 2.3 (curve g), and 2.5 GPa (curve h). As shown in Fig. 4(b), the imidazolium C–H absorptions appear at 3166 and 3198 $cm^{-1}$ corresponding to coupled $C^4$–H and $C^5$–H stretching vibrations. In comparison to $BMI^+BF_4^-$ [Figs. 2 and 4(a)], the coupled $C^4$–H and $C^5$–H bands of $BMM^+BF_4^-$ display similar nonmonotonic frequency shifts as the $BMM^+BF_4^-$ was compressed. The coupled $C^4$–H and $C^5$–H bands blue-shift initially [Figs. 4(b) and 4(c)], then undergoes no change [Figs. 4(c) and 4(d)], and then blue-shift again [Figs. 4(b)–4(h)]. On replacement of the H at $C^2$ with $CH_3$ in $BMM^+BF_4^-$, the hydrogen bonding interaction between the cation and the anion may be reduced. However, the unexpected increases in viscosities and melting points for $BMM^+$-based ionic liquids have been reported.[42,43] This finding suggests that the $C^4$–H and $C^5$–H groups can play non-negligible roles in ion pairs and clusters. This behavior is in accord with the pressure-dependent results [Figs. 2 and 4] indicating the similar trends observed for $C^2$–H, $C^4$–H, and $C^5$–H.

Figure 5 displays the infrared spectra of a $BMM^+BF_4^-$/DMSO-$d_6$ mixture having its mole fraction of $BMM^+BF_4^{--}$ equal to 0.14 obtained under ambient pressure (curve a), and at 0.3 (curve b), 0.9 (curve c), 1.5 (curve d), 1.9 (curve e), 2.3 (curve f), and 2.5 GPa (curve g). As revealed in Fig. 5(a), the imidazolium $C^4$–H and $C^5$–H stretching modes underwent changes as DMSO-$d_6$ was added, and the spectrum shows a broad band centered at about 3140 $cm^{-1}$ with a shoulder at 3085 $cm^{-1}$. The 3140 and 3085 $cm^{-1}$ bands can be assigned as isolated-(or dissociated-) C–H or isolated-C–H interacting with DMSO-$d_6$. As shown in Fig. 5(b), compression leads to a loss of isolated C–H band intensity. This observation indicates that imidazolium C–H hydrogen-bonded networks can be modified by varying the pressure, and the sharper structure of imidazolium C–H band at ca. 3164 $cm^{-1}$ revealed in Fig. 5(b) is in part due to the higher order and anisotropic environment in associated structures. The evolutions of the imidazolium C–H spectral features observed in Fig. 5 may arise from changes in local structures of $C^4$–H and $C^5$–H and the hydrogen-bond networks are likely perturbed by high pressures.

Figure 6 presents infrared spectra of a $BMM^+BF_4^-/D_2O$ mixture having mole fraction of $BMM^+BF_4^-$ equal to 0.06 obtained under ambient pressure (curve a), and at 0.3 (curve b), 0.9 (curve c), 1.5 (curve d), 1.9 (curve e), 2.3 (curve f), and 2.5 GPa (curve g). The C–H stretching absorptions overlap

with the O–H stretching bands of $H_2O$, so we measured the infrared spectra in a solution of $D_2O$, rather than $H_2O$ in Fig. 6. Looking into more detail in Fig. 6(a), we observe no drastic change in the concentration dependence of the imidazolium C–H spectral features. This behavior may suggest the association or clustering of $BMM^+BF_4^-$ in aqueous solutions and a slight perturbation by the presence of $D_2O$. This result is remarkably different from what is revealed for the imidazolium C–H groups in Fig. 5. The results of Fig. 6 also suggest that the associated structures are the favorable configurations up to the pressure of 2.5 GPa [Fig. 6(b)]. Recent investigations have suggested that the structure of ionic liquids exhibits spatial heterogeneity that results from their polar/nonpolar phase separation.[10,11,24] The association or aggregation of ionic liquids even in aqueous solution seems to be a general trend as revealed in Fig. 6. However, our results in Fig. 5 indicate that the presence of DMSO-$d_6$ significantly perturbs the ionic liquid–ionic liquid associations in the polar region.

We perform density functional theory (DFT) calculations using the GAUSSIAN program package.[44] Several stable complexes of $BMI^+/BMM^+$ with DMSO or ion pairs ($BMM^+BF_4^-$, $BMM^+BF_4^-$) with DMSO have been optimized. Figure S2 (Ref. 41) and Table I display some of the most stable DFT-calculated results of $BMI^+$DMSO [Figs. S2(a) and S2(b)], $BMM^+$DMSO [Figs. S2(c) and S2(d)], $BMI^+BF_4^-$DMSO [Figs. S2(e) and S2(f)], and $BMM^+BF_4^-$DMSO [Figs. S2(g) and S2(h)] complexes. We employed the B3LYP functional together with a standard 6–31+G* basis set. The geometry optimizations were made by analytical determinations of the first and second derivatives of the total energy. The energetically favored approach for the DMSO molecule to interact with the BMI+ cation is through the formation of $C^2$–H–O and $C^R$–H–O [Figs. S2(a) and S2(b); R denotes the alkyl group], whereas the former plays more important role due to the shorter distance. This fact could be related to the well-known acidity of $C^2$–H.[1,2] The substitution for a methyl group at the 2-position, i.e., $BMM^+$ cation, eliminates the hydrogen bonding interaction at $C^2$ [Figs. S2(c) and S2(d)], so C–H–O interactions are more favorable at $C^5$–H for Fig. S2(c) and at $C^4$–H for Fig. S2(d), respectively. The C–H–O distance in Fig. S2(a) (1.9386 Å) or Fig. S2(b) (1.9523Å) is a little shorter than that in Fig. S2(c) (2.0653 Å) or Fig. S2(d) (2.0658 Å), which reveals $C^2$–H–O interaction being stronger. Table I indicates that the interaction energy in $BMI^+$DMSO is larger than that in $BMM^+$DMSO by ca. 3 kcal/mol, and $C^4$–H (total interaction energy = 14.42 kcal/mol) is a slightly better proton donor than $C^5$–H (total interaction energy = 13.76 kcal/mol) due to steric effects of the butyl group adjacent to the $C^5$–H group and the positive inductive effect caused by the electron pushing butyl group.[45] This observation is in agreement with our experimental results in Fig. 5 indicating that $C^4$–H–O and $C^5$–H–O interactions seem to play non-negligible roles. As the anion ($BF_4^-$) is included in the calculation [see Figs. S2(e)–S2(h) and Table I], the interactions in complexes become complicated and the total interaction energy significantly increases due to the existence of more C–H–O and C–H–F interactions in $BMI^+BF_4^-$DMSO [Figs. S2(e) and S2(f)], and $BMM^+BF_4^-$DMSO [Figs. S2(g) and S2(h)] complexes. This behavior indicates that cohesion in ionic liquid is strong and the local organization between ionic species is preliminary governed by electrostatic interaction. The calculations of larger clusters may be interesting, but the number of low-lying isomers increases exponentially and the structural identification is complicated. Our calculations show that the total interactions energies in many stable optimized $BMI^+BF_4^-$DMSO and $BMM^+BF_4^-$DMSO complexes are close to ca. 90 and 85 kcal/mol, respectively. Figures 2(e)–2(h) illustrate that DMSO can interact with cation through the C–H–O interaction and interact with anion via C–H–F interactions.

TABLE I. Calculated relative energies (hartree/mol) and total interaction energies (kcal/mol)

| Species[a,b] | Relative energies | $-\Delta E$ |
|---|---|---|
| DMSO | −553.120468 | |
| $BF_4^-$ | −424.553137 | |
| $BMI^+$ | −422.959462 | |
| $BMM^+$ | −462.258348 | |
| a | −976.107254 | 16.66 |
| b | −976.108394 | 17.25 |
| c | −1015.401749 | 13.76 |
| d | −1015.402847 | 14.42 |
| e | −1400.779635 | 90.64 |
| f | −1400.779255 | 90.42 |
| g | −1440.075060 | 88.14 |
| h | −1440.072819 | 86.80 |

[a]Structures illustrated in Fig. S2.
[b]Numbering of the skeleton atoms for the $BMI^+$ cation.

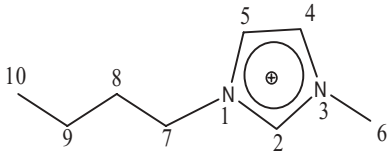


Figure 7 shows the Raman spectra in the region of C–D stretching of $BMI^+BF_4^-$/DMSO-$d_6$ mixture (curve a–g) and pure DMSO-$d_6$ (curve h), respectively. As revealed in Fig. 7(a), the spectrum has symmetric and asymmetric C–D stretching modes locating at 2143 and 2260 $cm^{-1}$, respectively, and the appearance of a shoulder at approximately 2116 $cm^{-1}$ should be attributed to the association of DMSO-$d_6$ with anions ($BF_4^-$) via C–D-F interactions. As the mixture was compressed, Figs. 7(b)–7(g) show the loss in intensity of the band at 2143 $cm^{-1}$. This observation suggests that the associated configuration via C–D–F is favored with increasing pressure by debiting the 2143 $cm^{-1}$ band. Figure 7(h) illustrates the experimental Raman spectrum of pure DMSO-$d_6$ obtained under the pressure of 2.5 GPa and the asymmetric C–D stretching mode becomes two separated bands at 2260 and 2278 $cm^{-1}$. In light of our previous report,[46] we anticipate that the high frequency component at 2278 $cm^{-1}$ is attributed to C–D–O interactions between neighboring DMSO-$d_6$ molecules or adjacent unit cells. In agreement with the prediction of our DFT-calculations, the Raman spectra suggest the non-negligible role of DMSO-anion association via C–H–F interaction. The S=O stretching frequencies at about 1000 $cm^{-1}$ should be a

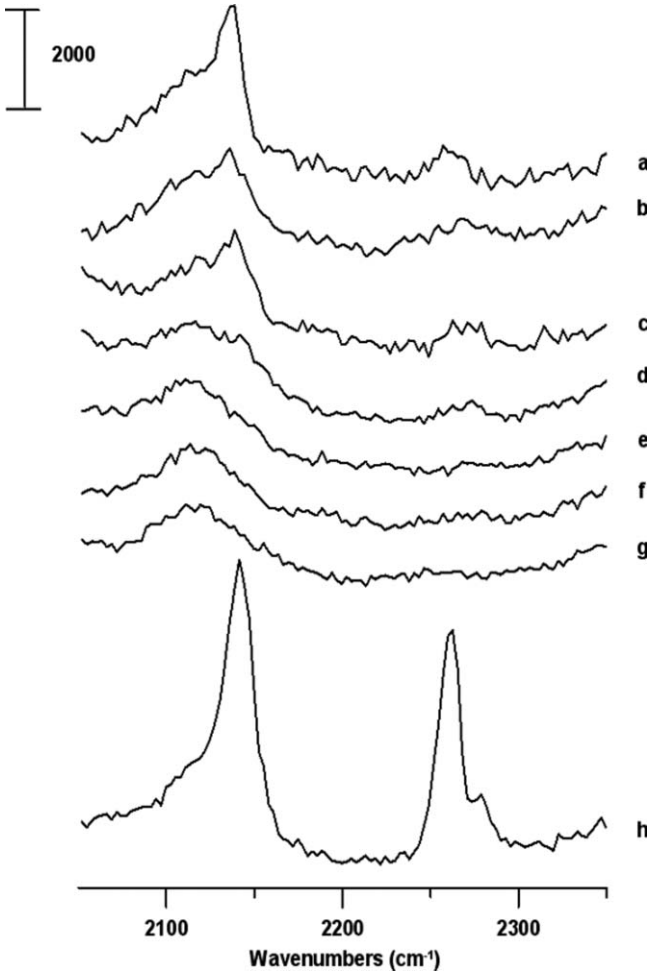


FIG. 7. Raman spectra of a $BMI^+BF_4^-$/DMSO-$d_6$ mixture (mole fraction of $BMI^+BF_4^-$: ca. 0.5) obtained under ambient pressure (curve a) and at 0.3 GPa (curve b), 0.9 GPa (curve c), 1.5 GPa (curve d), 1.9 GPa (curve e), 2.3 GPa (curve f) and 2.5 GPa (curve g). Curve h shows the C-D stretching of pure DMSO-$d_6$ under the pressure of 2.5 GPa.

sensitive probe for the interactions between cations and DMSO. Unfortunately, the S=O stretching absorption overlaps with the absorption of $BMI^+BF_4^-$ [Fig. 1(a) in Ref. 18].

## IV. CONCLUSION

The pressure-dependent behaviors for $BMI^+BF_4^-$/DMSO-$d_6$ and $BMM^+BF_4^-$/DMSO-$d_6$ mixtures exhibit transformations at high pressures including a transition from isolated configurations to associated forms. The associated forms are stable up to the pressure of 2.5 GPa. This observation indicates that imidazolium C–H hydrogen-bonded networks can be modified by varying the pressure. A possible explanation for this effect is the C–H–O interactions between imidazolium C–H groups and DMSO-$d_6$. Imidazolium C–H groups seem to be more favorable sites for C–H–O than the alkyl groups. In contrast to DMSO-$d_6$ mixtures, the local organization of imidazolium C–H groups in $D_2O$ mixtures is slightly perturbed by the presence of $D_2O$. Our DFT-calculations suggest that all imidazolium C–H groups, i.e., $C^2$–H, $C^4$–H, and $C^5$–H, play non-negligible roles.

## ACKNOWLEDGMENTS

The authors thank the National Dong Hwa University and the National Science Council (Contract No. NSC 98-2113-M-259-005-MY3) of Taiwan for financial support. The authors also thank Hou-Kuan Li and Yu-Fang Yeh for their assistance.

[1] *Ionic Liquids in Synthesis*, edited by P. Wasserscheid and T. Welton (Wiley VCH, Weinheim, 2008).
[2] H. Weingartner, Angew. Chem. Int. Ed. **47**, 654 (2008).
[3] E. W. Castner, Jr., J. F. Wishart, and H. Shirota, Acc. Chem. Res. **40**, 1217 (2007).
[4] C. Hardacre, J. D. Holbrey, M. Nieuwenhuyzen, and T. G. A. Youngs, Acc. Chem. Res. **40**, 1146 (2007).
[5] C. Schroder, T. Rudas, G. Neumayr, S. Benkner, and O. Steinhauser, J. Chem. Phys. **127**, 234503 (2007).
[6] D. Paschek, T. Koddermann, and R. Ludwig, Phys. Rev. Lett. **100**, 115901 (2008).
[7] L. Leclercq and A. R. Schmitzer, Supramol. Chem. **21**, 245 (2009).
[8] E. J. Maginn, J. Phys.: Condens. Matter **21**, 373101 (2009).
[9] B. Wu, Y. Liu, Y. Zhang, and H. Wang, Chem. Eur. J. **15**, 6889 (2009).
[10] U. Schroder, J. D. Wadhawan, R. G. Compton, F. Marken, P. A. Z. Suarez, C. S. Consorti, R. F. de Souza, and J. Dupont, New J. Chem. **24**, 1009 (2000).
[11] W. Jiang, Y. Wang, and G. A. Voth, J. Phys. Chem. B **111**, 4812 (2007).
[12] T. Koddermann, C. Wertz, A. Heintz, and R. Ludwig, Angew. Chem. Int. Ed. **45**, 3697 (2006).
[13] Y. Danten, M. I. Cabaco, and M. Besnard, J. Phys. Chem. A **113**, 2873 (2009).
[14] C. Spickermann, J. Thar, S. B. C. Lehmann, S. Zahn, J. Hunger, R. Buchner, P. A. Hunt, T. Welton, and B. Kirchner, J. Chem. Phys. **129**, 104505 (2008).
[15] H. C. Chang, J. C. Jiang, Y. C. Liou, C. H. Hung, T. Y. Lai, and S. H. Lin, J. Chem. Phys. **129**, 044506 (2008).
[16] T. Koddermann, C. Wertz, A. Heintz, and R. Ludwig, ChemPhysChem **7**, 944 (2006).
[17] S. A. Katsyuba, T. P. Griaznova, A. Vidis, and P. J. Dyson, J. Phys. Chem. B **113**, 5046 (2009).
[18] L. Zhang, Y. Wang, Z. Xu, and H. Li, J. Phys. Chem. B **113**, 5978 (2009).
[19] R. C. Remsing, Z. Liu, I. Sergeyev, and G. Moyna, J. Phys. Chem. B **112**, 7363 (2008).
[20] K. S. Mali, G. B. Dutt, and T. Mukherjee, J. Chem. Phys. **128**, 054504 (2008).
[21] R. Karmakar and A. Samanta, J. Phys. Chem. A **106**, 4447 (2002).
[22] J. H. Werner, S. N. Baker, and G.A. Baker, Analyst **128**, 786 (2003).
[23] S. Grundemann, A. Kovacevic, M. Albrecht, J. W. Faller, and R. H. Crabtree, Chem. Commun. (Cambridge) **21**, 2274 (2001).
[24] A. Triolo, O. Russina, H. Bleif, and E. Di Cola, J. Phys. Chem. B **111**, 4641 (2007).
[25] P. A. Hunt, B. Kirchner, and T. Welton, Chem. Eur. J. **12**, 6762 (2006).
[26] R. Katoh, M. Hara, and S. Tsuzuki, J. Phys. Chem. B **112**, 15426 (2008).
[27] S. G. Raju and S. Balasubramanian, J. Phys. Chem. B **113**, 4799 (2009).
[28] W. Zhao, F. Leroy, B. Heggen, S. Zahn, B. Kirchner, S. Balasubramanian, and F. Muller-Plathe, J. Am. Chem. Soc. **131**, 15825 (2008).
[29] A. Mele, C. D. Tran, and S. H. De Paoli Lacerda, Angew. Chem. Int. Ed. **42**, 4364 (2003).
[30] U. Domanska, E. Bogel-Lusaik, and R. Bogel-Lukasik, Chem.-Eur. J. **9**, 3033 (2003).
[31] Y. Umebayashi, J. C. Jiang, K. H. Lin, Y. L. Shan, K. Fujii, S. Seki, S. Ishiguro, S. H. Lin, and H. C. Chang, J. Chem. Phys. **131**, 234502 (2009).
[32] Y. Umebayashi, J. C. Jiang, Y. L. Shan, K. H. Lin, K. Fujii, S. Seki, S. Ishiguro, S. H. Lin, and H. C. Chang, J. Chem. Phys. **130**, 124503 (2009).
[33] H. C. Chang, J. C. Jiang, C. Y. Chang, J. C. Su, C. H. Hung, Y. C. Liou, and S. H. Lin, J. Phys. Chem. B **112**, 4351 (2008).
[34] P. Hobza and Z. Havlas, Chem. Rev. **100**, 4253 (2000).
[35] Y. L. Gu, T. Kar, and S. Scheiner, J. Am. Chem. Soc. **121**, 9411 (1999).

[36]A. Masunov, J. J. Dannenberg, and R. H. Contreras, J. Phys. Chem. A **105**, 4737 (2001).
[37]X. Li, L. Liu, and H. B. Schlegel, J. Am. Chem. Soc. **124**, 9639 (2002).
[38]K. Hermansson, J. Phys. Chem. A **106**, 4695 (2002).
[39]P. T. T. Wong, D. J. Moffatt, and F. L. Baudais, Appl. Spectrosc. **39**, 733 (1985).
[40]P. T. T. Wong and D. J. Moffatt, Appl. Spectrosc. **41**, 1070 (1987).
[41]See supplementary material at http://dx.doi.org/10.1063/1.3526485 for Figs. S1 and S2, respectively.
[42]P. A. Hunt, J. Phys. Chem. B **111**, 4844 (2007).
[43]I. B. Malham and M. Turmine, J. Chem. Thermodynamics **40**, 718 (2008).
[44]M. J. Frish, G. W. Trucks, H. B. Schlegel *et al.*, GAUSSIAN 03, Revision A.7, Gaussian Inc., Pittsburg, PA, 2003.
[45]H. Tokuda, K. Hayamizu, K. Ishii, Md. A.B.H. Susan, and M. Watanabe, J. Phys. Chem. B **109**, 6103 (2005).
[46]H. C. Chang, J. C. Jiang, C. M. Feng, Y. C. Yang, C. C. Su, P. J. Chang, and S. H. Lin, J. Chem. Phys. **118**, 1802 (2003).